Biochemical and Biophysical Research Communications 411 (2011) 82–87

Contents lists available at ScienceDirect

Biochemical and Biophysical Research Communications

journal homepage: www.elsevier.com/locate/ybbrc

Glutamate-induced metabolic changes influence the cytoplasmic redox state of hippocampal neurons

Omar H. Porras [a,*], Andrés Stutzin [a,b]

[a] Centro de los Estudios Moleculares de la Célula, CEMC, Facultad de Medicina Universidad de Chile, 8380453 Santiago, Chile
[b] Instituto de Ciencias Biomédicas, ICBM, Facultad de Medicina Universidad de Chile, 8380453 Santiago, Chile

ARTICLE INFO

Article history:
Received 9 June 2011
Available online 17 June 2011

Keywords:
Neurons
Lactate
Redox
Astrocytes
Glutamate
HyPer

ABSTRACT

Brain cell metabolism is intimately associated with intracellular oxidation–reduction (redox) balance. Glutamatergic transmission is accompanied with changes in substrate preference in neurons. Therefore, we studied cytoplasmatic redox changes in hippocampal neurons in culture exposed to glutamate. Neurons were transfected with HyPer, a genetically encoded redox biosensor for hydrogen peroxide which allows real-time imaging of the redox state. The rate of fluorescence decay, corresponding to the reduction of the biosensor was found to be augmented by low doses of glutamate (10 μM) as well as by pharmacological stimulation of NMDA glutamate receptors. Acute chelation of extracellular Ca^{2+} abolished the glutamate-induced effect observed on HyPer fluorescence. Additional experiments indicated that mitochondrial function and hence energetic substrate availability commands the redox state of neurons and is required for the glutamate effect observed on the biosensor signal. Furthermore, our results implicated astrocytic metabolism in the changes of neuronal redox state observed with glutamate.

1. Introduction

Cellular metabolism contributes directly to maintain redox homeostasis during oxidation of energetic substrates. Brain cells are particular in their metabolic behavior because, at rest they use glucose as the unique metabolite available for oxidation [1] whereas during glutamatergic transmission, neurons prefer lactate instead of glucose [2]. The physiological relevance of neuronal lactate consumption was established *in vivo* by knocking down cell-type specific isoforms of monocarboxylate transporters. This maneuver impaired long-term memory formation in intact rats [3], confirming previous *in vitro* and *in vivo* observations of metabolic preferences of astrocytes and neurons during glutamatergic activity [2,4–7].

Lactate metabolization is expected to increase the rate of oxidative phosphorylation in neuronal mitochondria, a notion supported by the fluctuations observed in the intrinsic NADH fluorescence measurements of hippocampal brain slices under electrical stimulation [6,8,9]. Considering the connection between metabolism and redox homeostasis, changes in neuronal metabolism will have an impact in the cellular redox balance. To investigate acute redox changes in neurons exposed to glutamate receptor activation we used the fluorescent ratiometric protein-based redox biosensor HyPer [10]. This biosensor belongs to a family of green or yellow fluorescent proteins (FPs) chosen as template to place cysteine pairs able to form disulfide bonds under oxidative environments thus changing their fluorescence properties [11], revised by Meyer and Dick [12]. Once a HyPer molecule is oxidized, its disulfide bond is susceptible to be reduced back to free thiol groups by the action of reducing mechanisms present in the cell. Based on these properties, we studied cytoplasmatic redox changes in living hippocampal neurons exposed to glutamate, as a redox switch has been proposed as a consequence of glutamate-induced metabolic adaptations [13]. Here, we demonstrate that glutamatergic stimulation reduces cysteine residues in HyPer supporting the notion of a redox switch. Furthermore, we demonstrate that these redox changes are dependent of mitochondrial function.

2. Materials and methods

2.1. Reagents and plasmids

DL-Lactate, Na^+-pyruvate, K^+-valinomycin, Na^+-monensin and standard chemicals were purchased from Sigma (St. Louis, MO). Fetal bovine serum, Minimal Essential Medium, trypsin, penicillin–streptomycin, Glutamax, Neurobasal and B27 supplement, lipo-

Abbreviations: NGF, neuronal growth factor; ROS, radical oxygen species; FBS, fetal bovine serum; DMEM, Dulbecco's modified eagle medium; $NMDG^+$, *N*-methyl D-glucamine$^+$; ANLS, astrocyte-neuron lactate shuttle; TMRM, tetra methyl rhodamine methyl ester; TRPM7, melastatin-type transient receptor potential channel 7.

* Corresponding author. Fax: +56 2 9786920.
E-mail address: oporras@bitmed.med.uchile.cl (O.H. Porras).

0006-291X/$ - see front matter © 2011 Elsevier Inc. All rights reserved.
doi:10.1016/j.bbrc.2011.06.097

fectamine 2000 and fluorescent probes (TMRM, Fluo4-AM and BCECF-AM) were purchased from Invitrogen (Carlsbad, CA, USA). Hydrogen peroxide was from Merck (Darmstadt, Germany). pHyPer-cito plasmid was purchased from Evrogen JSC (Moscow, Russia).

2.2. Brain cell culture

Sprague–Dawley rats were obtained from the Universidad de Chile; the entire animal procedure followed the protocol CBA #0264 FMUCH. Mixed cultures of brain cells were prepared from brains 1–3 days old neonates following the same indications as in Loaiza et al. [5]. Experiments were performed after 6 to 9 days in KRH buffer (in mM: 140 NaCl, 4.7 KCl, 20 HEPES, 1.25 $MgSO_4$ and 1.25 $CaCl_2$, pH 7.4).

2.3. PC12 cell culture

Rat pheochromocytoma PC12 cells (American Type Culture Collection) were cultured and differentiated as described in [14].

2.4. HyPer transfection and imaging

Lipofectamine 2000 or calcium phosphate [15] transfection method rendered similar low percent of transfected cells (~5% primary cultures). HyPer imaging was achieved by an inverted Olympus IX81 microscope with a 40× objective [numerical aperture, N.A. 1.3]. Cells were excited at 403/12 nm and 480/20 nm (MT20E emission wheel filter) and emission was detected at 555/28 nm with a CCD camera (XM10, Olympus). Experiments were conducted 24–48 h after transfection at room temperature (23–27 °C) in KRH buffer. A dose–response curve to exogenous H_2O_2 together with biosensor response to GSH 5 mM are shown in the Supplementary Fig. 1. Note that after H_2O_2 removal HyPer signal started to decay spontaneously likely because of disulfide bonds reduction in the biosensor by cytoplasmatic antioxidant systems present in neurons. The rate of decay was accelerated by addition of GSH 1 mM and 5 mM (Supplementary Fig. 1). For each experiment, pre-pulse of H_2O_2 duration was settled until HyPer signal reached a plateau.

Energetic depletion of glial cells was achieved by pre-incubating with fluoroacetate 5 mM for at least 3 h. This compound is only metabolized by astrocytes acting on aconitase stopping Krebs cycle [16,17]. At least 30 min before experiments started extracellular glucose was removed, thus glycogen becomes extinguished as the unique carbon source available. This protocol has been previously used to study the lactate transfer between astrocytes and neurons in hypothalamic slices from rats [18].

2.5. Mitochondrial potential, cytoplasmic Ca^{2+} and pH measurements

Mitochondrial potential was visualized by supplementing KRH with tetramethyl-rhodamine methyl ester (TMRM, 20 nM). Astrocytic from neuronal mitochondria were distinguished by collecting the light from different focal planes (Supplemental Fig. 2). TMRM was excited at 565/25 nm and emitted light was collected with a long pass filter 617 nm. For calcium imaging, cells were loaded with the fluorescent cell-permeant calcium indicator Fluo-4 at 5 μM for 30 min in KRH-glc containing 0.02% pluronic acid followed by 20 min of de-esterification time. Fluo-4 was imaged at 480/20 nm excitation and emission was collected at 555/28 nm. For the intracellular pH measurements cells were loaded with 2′,7′-bis-(2-carboxyethyl)-5-(and-6)-carboxyfluorescein (BCECF) at 0.5 μM in its esterificated form for 5 min in KRH-glc containing 0.02% pluronic acid. Cells were allowed to de-esterify for at least 30 min and BCECF calibration was performed as described in [19] with the exception that valinomycin 25 μM was used instead of gramicidin. Intracellular pH recording was carried out to discern the contribution of glutamate-dependent acidification on HyPer signal decay. Glutamate (10 μM) exposure resulted in a drop of 0.1 pH units at neuronal cytoplasm within relevant time window of HyPer fluctuations reported here (~150 s), whereas controlled drop of 0.5 pH units rendered a HyPer ratio drop of 0.8 units, therefore glutamate-dependent acidification is insufficient to explain the magnitude of HyPer signal changes observed here.

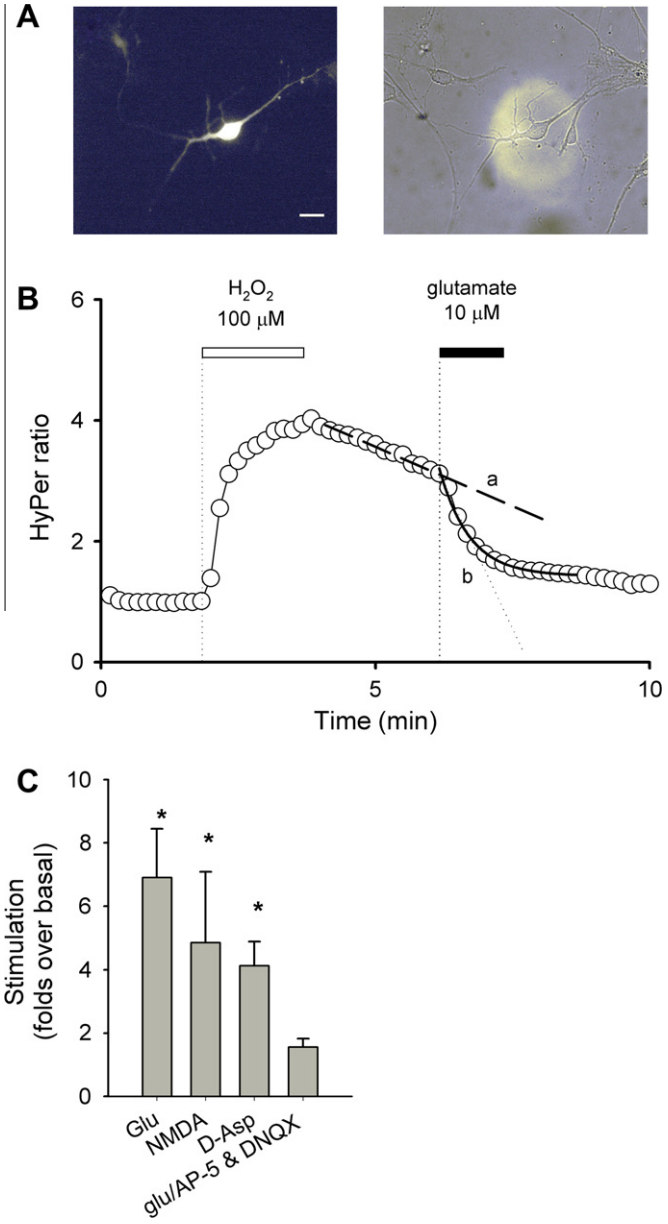

Fig. 1. Glutamate receptors stimulation accelerates the HyPer signal decay in neurons. (A), cytoplasmic expression of HyPer is shown in a neuron 48 h post-transfection together with its correspondent bright field image. White scale bar corresponds to 20 μm. (B), time-course of HyPer ratio from a neuron, biosensor was pre-oxidized with H_2O_2 100 μM (white bar). After H_2O_2 removal, the signal spontaneously decays with a slope *a*, following a lineal behavior. Upon glutamate exposure (10 μM, black bar) the decay accelerates with a slope *b*, in an exponential fashion. (C), a summary plot showing the fold of stimulation in the slope a versus slope b at different conditions: Glutamate (Glu, 10 μM, $n = 21$), NMDA (200 μM, $n = 8$), D-Aspartate (D-Asp, 10 μM, $n = 4$) and glutamate in the presence of 2R-amino-5-phosphonovaleric acid (10 μM) and 6,7-dinitroquinoxaline-2,3-dione (10 μM) (glu/AP-5&DNQX, $n = 7$). The asterisks mean statistical significance.

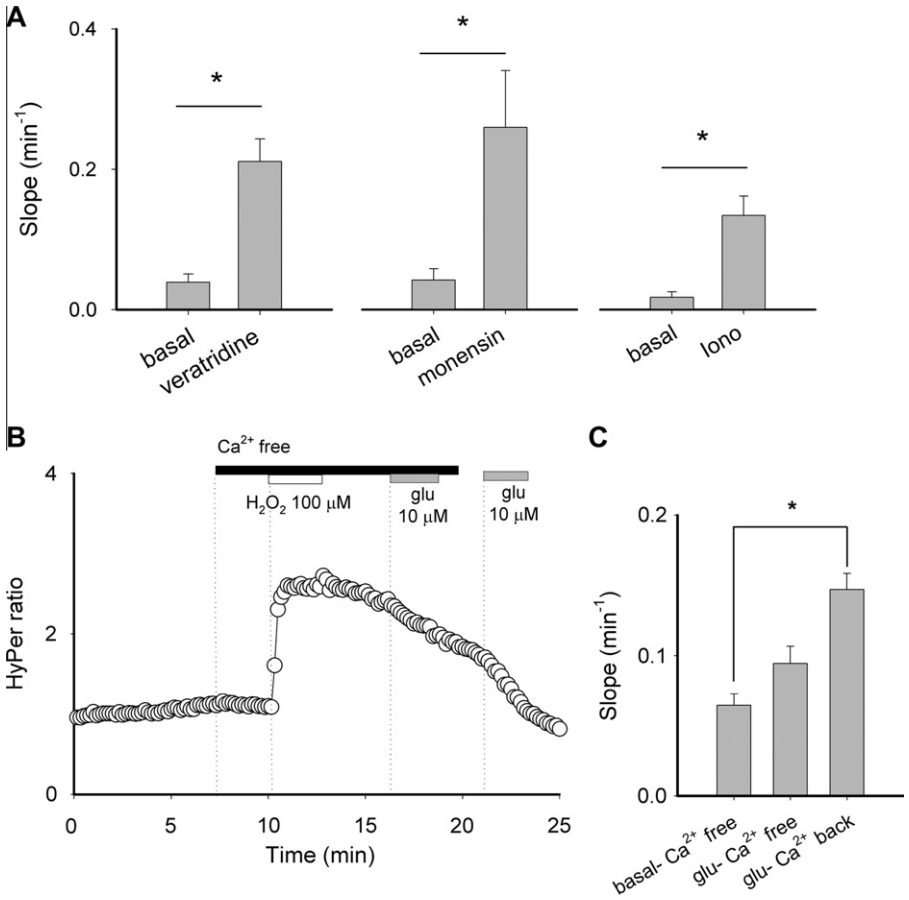

Fig. 2. Calcium influx is sufficient and necessary to glutamate-evoked HyPer signal diminishment. (A), Comparative bar graphs showing slopes at basal conditions versus decay rates obtained by veratridine (75 μM, $n = 5$), monensin (100 μM, $n = 10$)) and ionomycin (iono, 2 μM. $n = 8$). The asterisks mean the statistically significance obtained by paired t-test. (B), cytoplasmic HyPer ratio recording was carried out in a Ca^{2+} free-buffer supplemented with EGTA 5 mM (black bar). After H_2O_2 pre-pulse (white bar), glutamate 10 μM was added in the absence of external calcium (first gray bar). A second application of glutamate was executed in the presence of extracellular Ca^{2+} (last gray bar). (C), graph bar summarizing 9 experiments. The asterisk means the statistical significance obtained by RM-ANOVA test.

2.6. Statistical analysis

Regression analysis and data fitting were carried out with Sigmaplot 5.0 (Jandel Corporation, Erkrath, Germany). Data are presented as means ± SEM. Differences in mean values were evaluated with paired Student's t-test for comparisons of before and after treatments and repeated measurement ANOVA (RM-ANOVA) when more than two conditions were present during the experiment.

3. Results

3.1. Glutamate induces a rapid decrease in HyPer fluorescent signal in hippocampal neurons

We decided to investigate whether known metabolic adaptations that occur in neurons by glutamatergic transmission are also accompanied by cytoplasmic redox state fluctuations. To avoid the natural variance of neurons at basal conditions, we followed the idea to apply a short pre-pulse of H_2O_2 100 μM. After H_2O_2 removal, a slow and constant decrease of HyPer fluorescence could be quantified by simple linear fitting rendering a basal rate of $0.04 \pm 0.01\ min^{-1}$ (slope a, Fig. 1B). However, upon glutamate (10 μM) exposure, HyPer signal decay was accelerated (slope b in Fig. 1B). This effect was found in ~80% of the neurons studied and in average the neurotransmitter increased the slope by seven fold (Fig. 1C). As a control, glutamate was assayed in transfected HEK cells with no effect on HyPer signal, indicating that exclusive glutamate sensing by neurons is necessary (data not shown).

We tested next whether pharmacological stimulation of NMDA-sensitive glutamate receptors could mimic the glutamate effect observed above. As shown in Fig. 1C, *N*-methyl-D-aspartate (200 μM) and D-aspartate (10 μM) were equally effective as glutamate in accelerating the decrease of the HyPer signal. Accordingly, pretreatment with the ionotropic glutamate receptor blockers, amino-5-phosphonovaleric acid and 6,7-dinitroquinoxaline-2,3-dione, prevented the glutamate effect on HyPer signal (Fig. 1C). These results suggest that activation of NMDA-sensitive glutamate receptors is involved in the mechanisms that connect glutamate sensing with the increase in the reducing tone in neuronal cytoplasm.

Ionotropic glutamate receptor activation, particularly NMDA-sensitive receptors, leads to Na^+ and Ca^{2+} influx. In order to bypass complex molecular signals triggered by glutamate receptor activation, we tested whether an independent Ca^{2+} entry could trigger a reduction in the biosensor fluorescence as well. To that end, we treated neurons with veratridine, monensin and ionomycin (Fig. 2A). The first two compounds induce a cytoplasmic Na^+ load, with the concomitant opening of voltage dependent channels among those, Ca^{2+} permeant channels, whereas ionomycin increases Ca^{2+} permeability by itself. All of three compounds were able to increase the slope of HyPer signal decay significantly. For further confirmation of Ca^{2+} influx as mediator in the glutamate effect, we performed experiments with a Ca^{2+}-free solution plus

5 mM EGTA (Fig. 2B). Under this condition, glutamate was unable to evoke a decrease in biosensor ratio. However, the glutamate effect was reestablished upon Ca^{2+} reintroduction to the extracellular media (Fig. 2B and C). Together, these results indicate that Ca^{2+} influx is a central component in the glutamate-evoked reduction of the biosensor in the cytoplasmatic neuronal environment.

It is important to emphasize the effect obtained with monensin because it helps to exclude intracellular acidification as a factor in the HyPer signal decay observed with glutamate. Because monensin is a Na^+/H^+ antiporter, cytoplasmic Na^+ load is accompanied by proton extrusion. Therefore, an alkalinization must occur at the cytoplasmic compartment, a pH shift opposite to the acidification expected with glutamate (Supplemental Fig. 3).

3.2. The astrocytic metabolism is connected with the neuronal redox status

Intriguingly, the decline in the fluorescence signal of HyPer either induced by ionophore-induced Ca^{2+} influx or by glutamate exposure could be observed in the absence of any metabolic fuel (e.g. glucose). Considering that neurons do not store glycogen, it is reasonable to assume that after ten minutes without glucose the glycolytic flux had diminished to negligible levels. However, mitochondria still can produce reducing equivalents by feeding the Krebs cycle with intermediaries. To unveil the mitochondrial machinery involved in the metabolic response evoked by glutamate, we studied simultaneously mitochondrial potential of neurons and astrocytes by means of the cationic fluorescent probe TMRM. As can be observed in Fig. 3A, glutamate evoked opposite responses from neurons and astrocytes. In neurons, mitochondrial potential transiently increased likely due to increased oxidative phosphorylation. However, in astrocytes mitochondrial potential slightly decreased. This glutamate-evoked metabolic adaptation in neurons occurs in the same temporal window of glutamate-evoked HyPer signal decline, suggesting that glutamate increases mitochondrial function boosting the reducing potential of neurons. To determine the role of mitochondria, we switched off mitochondrial function with antimycin A (0.25 μg/ml). Under this condition, glutamate was unable to affect the biosensor fluorescence (Fig. 3B and C), suggesting that mitochondrial function is part of the metabolic adaptation necessary for glutamate to increase the reducing potential at the cytoplasm of hippocampal neurons.

To investigate whether astrocytic metabolism is connected with neuronal glutamate-dependent redox changes, glial metabolism was specifically impaired with fluoroacetate (5 mM). Fig. 4A shows a time course of HyPer signal recorded from a single neuron from a plate with astrocytes energetically deprived. As depicted, this condition was effective in avoiding the glutamate effect on HyPer described before. No significant changes in the basal rate of HyPer recovery before and after glutamate exposure were detected. Moreover, the addition of exogenous lactate at the end of the experiment resulted in a slight acceleration in the rate of decay in HyPer fluorescence, further experiments were performed on neurons to validate the effectivity of lactate (1, 2 and 5 mM) and pyruvate (10 mM) to augment the decay rate of HyPer signal in neurons (Supplemental Fig. 4A). These findings indicate that astrocytic metabolic machinery is pivotal in the decrease of the HyPer ratio at neurons and that, the availability of energetic substrates at media (e.g. lactate or pyruvate) also affect the cellular redox state.

To explore the transfer of energy substrates, we switched to PC12 cells, a cell line that can be differentiated to a neuronal phenotype with NGF [20]. Initially, the dose of glutamate (10 μM) used on neurons during this study was ineffective to trigger an intracellular Ca^{2+} rise in differentiated PC12 cells and thus, higher doses, 0.1 and 1 mM, were tried and their effectivity to mobilize Ca^{2+} was confirmed by calcium imaging (not shown). As depicted in

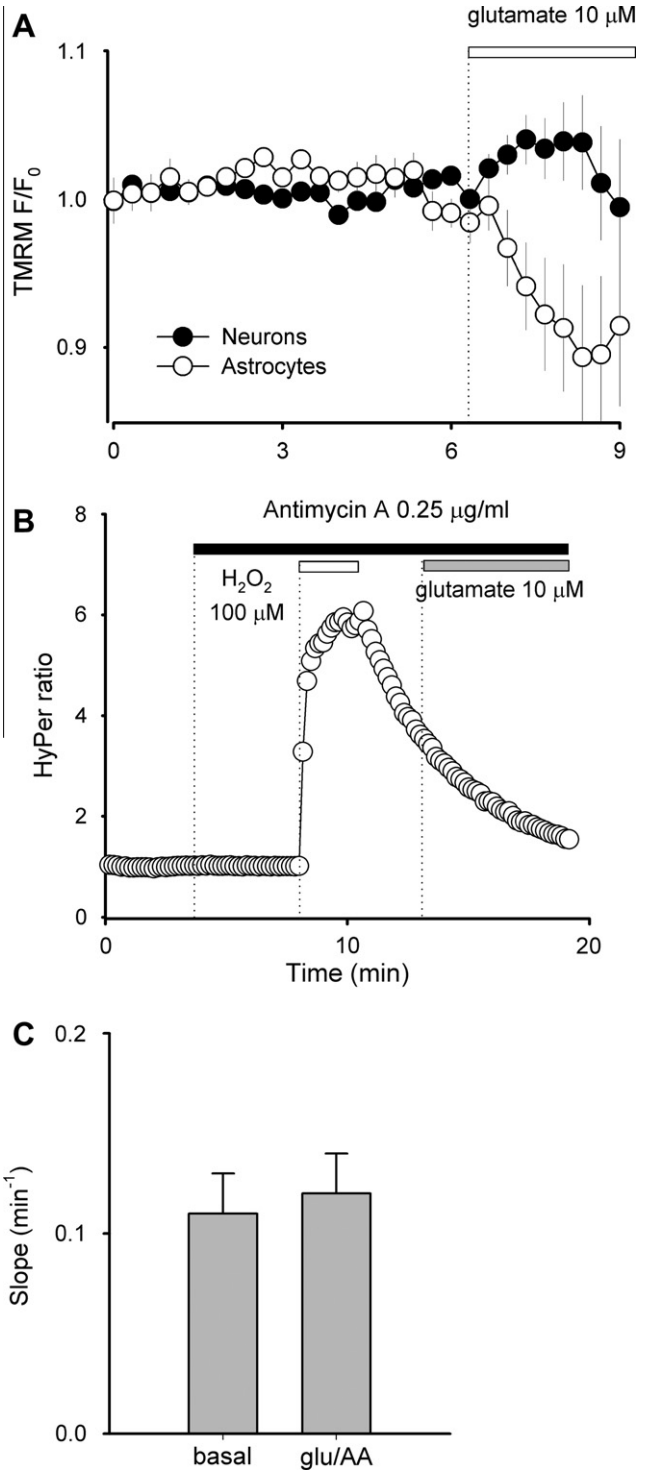

Fig. 3. Mitochondrial function is differentially affected in neurons and astrocytes and, is required by glutamate to decrease HyPer signal in neurons. (A), mitochondrial potential was simultaneously imaged in astrocytes and neurons by incubating the cell preparation with TMRM 20 nM. Glutamate exposure is indicated by the white bar. Data correspond to the average ± SEM of 4 neurons (filled circles) and 4 astrocytes (empty circles). This experiment is representative of other two. (B), HyPer signal recorded from a transfected neuron treated with antimycin A (black bar, 0.25 μg/ml). The glutamate exposure (gray bar, 10 μM) did not accelerate the basal slope of fluorescence recovery obtained after hydrogen peroxide removal. A summary of the results from eight independent experiments is shown in (C).

Fig. 4C, both doses of glutamate showed to be ineffective at decreasing the HyPer fluorescence. However, adding lactate resulted in a drop in the HyPer signal with similar characteristics

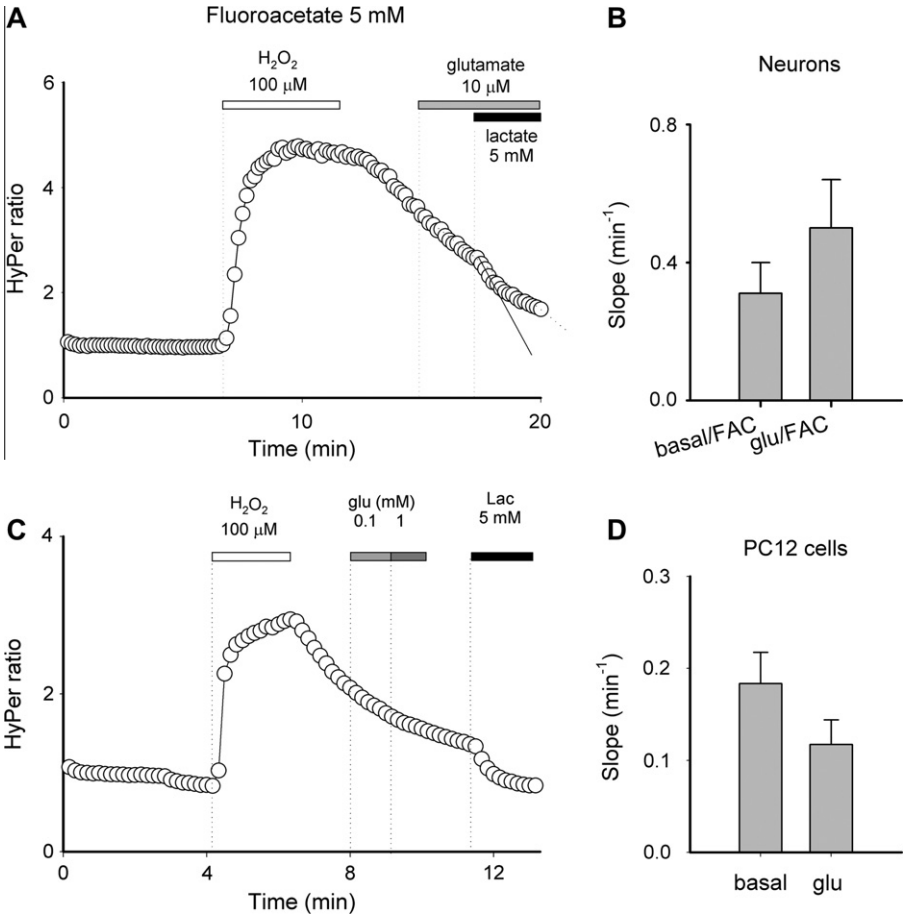

Fig. 4. Astrocytes are pivotal for glutamate-induced redox changes in neurons. (A), at day of the experiment cells were pre-incubated with fluoroacetate (5 mM) and HyPer ratio was imaged. After H_2O_2 pre-pulse (white bar, 100 μM), glutamate 10 μM (gray bar) was applied. (B), data from eight experiments were summarized in bar graph. (C), time-course of HyPer ratio was recorded from a single NGF-differentiated PC12 cell. Similar to A, a H_2O_2 pre-pulse was applied (white bar) to then, apply glutamate (0.1 and 1 mM, gray and dark gray bars, respectively). At the end of the time-course, lactate 5 mM was added (black bar). (D), comparison between the slopes before and after glutamate exposure of three independent experiments is plotted.

as those evoked by glutamate in neurons. Additional experiments corroborated that the sole addition of lactate 5 mM induced an accelerated decay in HyPer fluorescence (Supplemental Fig. 4B). These results strongly suggest that although differentiated PC12 cells exhibit the glutamate-sensing machinery, glutamate-induced redox changes require extra-neuronal (PC12 cells) factor(s) to evoke an increase in PC12 cytoplasmic reducing capacity. The effects of those energetic substrates on the reducing tone confirm that the availability of energetic substrates has an impact on the cellular redox state.

4. Discussion

The Astrocyte Neuron Lactate Shuttle (ANLS) hypothesis was first proposed in 1994 and by now, is widely accepted [2–5,7,21]. Our investigation has added the cytoplasmic redox homeostasis as a new cellular aspect that is modified as consequence of glutamate-evoked metabolic changes in neurons and that this neuronal feature depends on the astrocytic metabolism. The later is supported by the lack of effect obtained in co-cultures treated with fluoroacetate and the vast evidence supporting the orchestrating role of glutamate in the metabolic coupling between neurons and astrocytes [3,4,9,22–25].

Our results indicate that an accelerated reduction of disulfide bonds present in the HyPer molecule depends of glutamate-stimulated mitochondrial metabolism. Perhaps in contraposition to the generalized notion of mitochondria as the major cellular ROS source, an idea based on measurements of H_2O_2 production from mitochondria powered by succinate at non-physiological oxygen conditions [26]. Now, considering that even under this "forced" conditions H_2O_2 accounts only for 1–2% of the total oxygen consumption in liver mitochondria, this organelle must be considered highly efficient [27]. Zoccarato et al. showed that energized mitochondria are twenty-fold more efficient to remove extra-mitochondrial H_2O_2 than de-energized, suggesting that high metabolic activity is translated to enhanced ROS scavenging [28]. At the contrary, simultaneous imaging of mitochondria depolarization and cytoplasmic GSH in HeLa cells showed a reciprocal relationship between those parameters [11]. In line with this observation, we observed that stimulated mitochondrial function is translated to an enhanced reducing tone at neuronal cytoplasm. Evidently, efficient mechanisms implicated in the redox transfer between mitochondrial and cytoplasmic compartments must occur [29–31]. Noteworthy, Ca^{2+} signaling might be working as a feed-forward mechanism to prepare neurons to efficiently metabolize lactate and pyruvate. In beating cardiomyocytes, for instance, elevations in cytoplasmic Ca^{2+} are sensed by mitochondrial-targeted aequorin [32], Ca^{2+} oscillations are well known stimulating factors of oxidative metabolism by stimulation of mitochondrial dehydrogenase enzymes with the concomitant increase in NADH [33] and ATP production [32].

Our experimental strategy of pre-oxidizing the biosensor with a H_2O_2 pulse deserves some attention for the possible undesired ef-

fects on brain cell metabolism. Since glutamate-evoked redox changes reported here were found in absence of extracellular glucose, glycogen breakdown and lactate efflux must be considered instead. Glycogen mobilization is accelerated by 2.5-fold in the presence of 200 μM of H_2O_2 [34], however, the hydrogen peroxide-stimulated half-time of 16 min is too slow to influence the redox variations reported here. Lactate release, on the other hand, is not affected by H_2O_2 in the temporal window relevant for this study. For instance, lactate release from brain slices does not change by one hour with identical H_2O_2 concentration used here [35] and in cultured cortical astrocytes, lactate efflux diminished only slightly when glia was exposed to a H_2O_2-generating system for 30 min, an opposite response compared with the typical stimulation reported with glutamate. Additionally, H_2O_2 pre-pulse did not affect the Ca^{2+} homeostasis in our system, supporting that short duration and low H_2O_2 concentration used were safe enough to avoid undesired effects.

A redox shift towards a more reducing tone at the cytoplasm under glutamatergic transmission could serve as a mechanism to guarantee proper membrane repolarization [36], glutamate re-uptake [37] and avoid Ca^{2+} homeostasis deregulation by S-glutathionylation of ryanodine isoform 2 channels [38] and activation of TRPM7-mediated inwards a currents, which otherwise could lead to excitotoxicity [39]. In summary, we propose that redox shift towards a more reducing tone due to glutamate-dependent metabolic plasticity might be also serving as a protective mechanism during neuronal transmission.

Acknowledgments

The authors are grateful to L. Felipe Barros for suggestions and critically reading the manuscript. PC12 cells were kindly provided by Felipe Simon. This work was supported by grant 15010006 from Fondecyt-FONDAP (Fondo de Financiamiento de Centros de Excelencia en Investigación) (AS) and grant 3090030 from Fondecyt-Postdoctoral (to OP).

Appendix A. Supplementary data

Supplementary data associated with this article can be found, in the online version, at doi:10.1016/j.bbrc.2011.06.097.

References

[1] L. Sokoloff, Relation between physiological function and energy metabolism in the central nervous system, J. Neurochem. 29 (1977) 13–26.
[2] O.H. Porras, A. Loaiza, L.F. Barros, Glutamate mediates acute glucose transport inhibition in hippocampal neurons, J. Neurosci. 24 (2004) 9669–9673.
[3] A. Suzuki, S.A. Stern, O. Bozdagi, G.W. Huntley, R.H. Walker, P.J. Magistretti, C.M. Alberini, Astrocyte-neuron lactate transport is required for long-term memory formation, Cell 144 (2011) 810–823.
[4] L. Pellerin, P.J. Magistretti, Glutamate uptake into astrocytes stimulates aerobic glycolysis: a mechanism coupling neuronal activity to glucose utilization, Proc. Natl. Acad. Sci. USA 91 (1994) 10625–10629.
[5] A. Loaiza, O.H. Porras, L.F. Barros, Glutamate triggers rapid glucose transport stimulation in astrocytes as evidenced by real-time confocal microscopy, J. Neurosci. 23 (2003) 7337–7342.
[6] K.A. Kasischke, H.D. Vishwasrao, P.J. Fisher, W.R. Zipfel, W.W. Webb, Neural activity triggers neuronal oxidative metabolism followed by astrocytic glycolysis, Science 305 (2004) 99–103.
[7] L.F. Barros, R. Courjaret, P. Jakoby, A. Loaiza, C. Lohr, J.W. Deitmer, Preferential transport and metabolism of glucose in Bergmann glia over Purkinje cells: a multiphoton study of cerebellar slices, Glia 57 (2009) 962–970.
[8] A.M. Brennan, J.A. Connor, C.W. Shuttleworth, NAD(P)H fluorescence transients after synaptic activity in brain slices: predominant role of mitochondrial function, J. Cereb. Blood Flow Metab. 26 (2006) 1389–1406.
[9] R.G. Shulman, F. Hyder, D.L. Rothman, Lactate efflux and the neuroenergetic basis of brain function, NMR Biomed. 14 (2001) 389–396.
[10] V.V. Belousov, A.F. Fradkov, K.A. Lukyanov, D.B. Staroverov, K.S. Shakhbazov, A.V. Terskikh, S. Lukyanov, Genetically encoded fluorescent indicator for intracellular hydrogen peroxide, Nat. Methods 3 (2006) 281–286.
[11] M. Gutscher, A.L. Pauleau, L. Marty, T. Brach, G.H. Wabnitz, Y. Samstag, A.J. Meyer, T.P. Dick, Real-time imaging of the intracellular glutathione redox potential, Nat. Methods 5 (2008) 553–559.
[12] A.J. Meyer, T.P. Dick, Fluorescent protein-based redox probes, Antioxid. Redox. Signal. 13 (2010) 621–650.
[13] S. Cerdan, T.B. Rodrigues, A. Sierra, M. Benito, L.L. Fonseca, C.P. Fonseca, M.L. Garcia-Martin, The redox switch/redox coupling hypothesis, Neurochem. Int. 48 (2006) 523–530.
[14] F. Nunez-Villena, A. Becerra, C. Echeverria, N. Briceno, O. Porras, R. Armisen, D. Varela, I. Montorfano, D. Sarmiento, F. Simon, Increased expression of the transient receptor potential melastatin 7 channel is critically involved in lipopolysaccharide-induced ROS-mediated neuronal death, Antioxid. Redox. Signal. (2011).
[15] M. Jiang, G. Chen, High Ca^{2+}-phosphate transfection efficiency in low-density neuronal cultures, Nat. Protoc. 1 (2006) 695–700.
[16] D. Muir, S. Berl, D.D. Clarke, Acetate and fluoroacetate as possible markers for glial metabolism in vivo, Brain Res. 380 (1986) 336–340.
[17] D.D. Clarke, Fluoroacetate and fluorocitrate: mechanism of action, Neurochem. Res. 16 (1991) 1055–1058.
[18] M.P. Parsons, M. Hirasawa, ATP-sensitive potassium channel-mediated lactate effect on orexin neurons: implications for brain energetics during arousal, J. Neurosci. 30 (2010) 8061–8070.
[19] J. Castro, C.X. Bittner, A. Humeres, V.P. Montecinos, J.C. Vera, L.F. Barros, A cytosolic source of calcium unveiled by hydrogen peroxide with relevance for epithelial cell death, Cell Death. Differ. 11 (2004) 468–478.
[20] M. Casado, A. Lopez-Guajardo, B. Mellstrom, J.R. Naranjo, J. Lerma, Functional *N*-methyl-D-aspartate receptors in clonal rat phaeochromocytoma cells, J. Physiol. 490 (Pt 2) (1996) 391–404.
[21] O.H. Porras, I. Ruminot, A. Loaiza, L.F. Barros, Na(+)-Ca(2+) cosignaling in the stimulation of the glucose transporter GLUT1 in cultured astrocytes, Glia 56 (2008) 59–68.
[22] K. Caesar, P. Hashemi, A. Douhou, G. Bonvento, M.G. Boutelle, A.B. Walls, M. Lauritzen, Glutamate receptor-dependent increments in lactate, glucose and oxygen metabolism evoked in rat cerebellum in vivo, J. Physiol. 586 (2008) 1337–1349.
[23] R.G. Shulman, F. Hyder, D.L. Rothman, Cerebral energetics and the glycogen shunt: neurochemical basis of functional imaging, Proc. Natl. Acad. Sci. USA 98 (2001) 6417–6422.
[24] M.E. Gibbs, D.G. Anderson, L. Hertz, Inhibition of glycogenolysis in astrocytes interrupts memory consolidation in young chickens, Glia 54 (2006) 214–222.
[25] C.X. Bittner, R. Valdebenito, I. Ruminot, A. Loaiza, V. Larenas, T. Sotelo-Hitschfeld, H. Moldenhauer, M.A. San, R. Gutierrez, M. Zambrano, L.F. Barros, Fast and reversible stimulation of astrocytic glycolysis by k+ and a delayed and persistent effect of glutamate, J. Neurosci. 31 (2011) 4709–4713.
[26] A. Boveris, N. Oshino, B. Chance, The cellular production of hydrogen peroxide, Biochem. J. 128 (1972) 617–630.
[27] A.P. Kudin, D. Malinska, W.S. Kunz, Sites of generation of reactive oxygen species in homogenates of brain tissue determined with the use of respiratory substrates and inhibitors, Biochim. Biophys. Acta 1777 (2008) 689–695.
[28] F. Zoccarato, M. Cappellotto, A. Alexandre, Clorgyline and other propargylamine derivatives as inhibitors of succinate-dependent $H_{(2)}O_{(2)}$ release at NADH:UBIQUINONE oxidoreductase (Complex I) in brain mitochondria, J. Bioenerg. Biomembr. 40 (2008) 289–296.
[29] M.C. McKenna, H.S. Waagepetersen, A. Schousboe, U. Sonnewald, Neuronal and astrocytic shuttle mechanisms for cytosolic-mitochondrial transfer of reducing equivalents: current evidence and pharmacological tools, Biochem. Pharmacol. 71 (2006) 399–407.
[30] C.E. Outten, V.C. Culotta, A novel NADH kinase is the mitochondrial source of NADPH in Saccharomyces cerevisiae, EMBO J. 22 (2003) 2015–2024.
[31] N. Pollak, M. Niere, M. Ziegler, NAD kinase levels control the NADPH concentration in human cells, J. Biol. Chem. 282 (2007) 33562–33571.
[32] C.J. Bell, N.A. Bright, G.A. Rutter, E.J. Griffiths, ATP regulation in adult rat cardiomyocytes: time-resolved decoding of rapid mitochondrial calcium spiking imaged with targeted photoproteins, J. Biol. Chem. 281 (2006) 28058–28067.
[33] C. Garcia-Perez, G. Hajnoczky, G. Csordas, Physical coupling supports the local Ca^{2+} transfer between sarcoplasmic reticulum subdomains and the mitochondria in heart muscle, J. Biol. Chem. 283 (2008) 32771–32780.
[34] B. Rahman, L. Kussmaul, B. Hamprecht, R. Dringen, Glycogen is mobilized during the disposal of peroxides by cultured astroglial cells from rat brain, Neurosci. Lett. 290 (2000) 169–172.
[35] L.M. Vieira de Almeida, C.C. Pineiro, M.C. Leite, G. Brolese, R.B. Leal, C. Gottfried, C.A. Goncalves, Protective effects of resveratrol on hydrogen peroxide induced toxicity in primary cortical astrocyte cultures, Neurochem. Res. 33 (2008) 8–15.
[36] H. Soh, W. Jung, D.Y. Uhm, S. Chung, Modulation of large conductance calcium-activated potassium channels from rat hippocampal neurons by glutathione, Neurosci. Lett. 298 (2001) 115–118.
[37] J.Y. Yun, K.S. Park, J.H. Kim, S.H. Do, Z. Zuo, Propofol reverses oxidative stress-attenuated glutamate transporter EAAT3 activity: evidence of protein kinase C involvement, Eur. J. Pharmacol. 565 (2007) 83–88.
[38] R. Bull, J.P. Finkelstein, J. Galvez, G. Sanchez, P. Donoso, M.I. Behrens, C. Hidalgo, Ischemia enhances activation by Ca^{2+} and redox modification of ryanodine receptor channels from rat brain cortex, J. Neurosci. 28 (2008) 9463–9472.
[39] M. Aarts, K. Iihara, W.L. Wei, Z.G. Xiong, M. Arundine, W. Cerwinski, J.F. MacDonald, M. Tymianski, A key role for TRPM7 channels in anoxic neuronal death, Cell 115 (2003) 863–877.